View metadata, citation and similar papers at core.ac.uk
brought to you by CORE
provided by ScholarWorks@UNIST

*Int. J. Electrochem. Sci.*, 8 **(2013)** 8272 - 8281

International Journal of
ELECTROCHEMICAL
SCIENCE
www.electrochemsci.org

# Electrochemical Investigation of High-Performance Dye-Sensitized Solar Cells Based on Molybdenum for Preparation of Counter Electrode

*Kyoseung Sim*[1], *Shi-Joon Sung*[1*], *Hyo Jeong Jo*[2], *Dong-Hwan Jeon*[3], *Dae-Hwan Kim*[1], *Jin-Kyu Kang*[1,2,*]

[1] Green Energy Research Division, Daegu Gyeongbuk Institute of Science & Technology (DGIST), 50-1, Sang-ri, Hyeonpung-myeon, Dalseong-gun, Daegu, 711-873, Republic of Korea
[2] Advanced Convergence Research Center, Daegu Gyeongbuk Institute of Science & Technology (DGIST), 50-1, Sang-ri, Hyeonpung-myeon, Dalseong-gun, Daegu, 711-873, Republic of Korea
[3] Robotics Research Division, Daegu Gyeongbuk Institute of Science & Technology (DGIST), 50-1, Sang-ri, Hyeonpung-myeon, Dalseong-gun, Daegu, 711-873, Republic of Korea
[*]E-mail: sjsung@dgist.ac.kr; apollon@dgist.ac.kr

*Received:* 13 March 2013 / *Accepted:* 24 April 2013 / *Published:* 1 June 2013

In order to improve the photocurrent conversion efficiency of dye-sensitized solar cells (DSSCs), we studied an alternative conductor for the counter electrode and focused on molybdenum (Mo) instead of conventional fluorine-doped tin oxide (FTO). Because Mo has a similar work function to FTO for band alignment, better formability of platinum (Pt), and a low electric resistance, using a counter electrode made of Mo instead of FTO lead to the enhancement of the catalytic reaction of the redox couple, reduce the interior resistance of the DSSCs, and prevent energy-barrier formation. Using electrical measurements under a 1-sun condition (100 mW/cm$^2$, AM 1.5), we determined that the fill factor (*FF*) and photocurrent conversion efficiency ($\eta$) of DSSCs with a Mo electrode were respectively improved by 7.75% and 5.59% with respect to those of DSSCs with an FTO electrode. Moreover, we have investigated the origin of the improved performance through surface morphology analyses such as scanning electron microscopy and electrochemical analyses including cyclic voltammetry and impedance spectroscopy.

**Keywords:** Molybdenum, Electrocatalytic activity, Electrochemical analysis, Counter electrode, Dye-sensitized solar cells**.**

## 1. INTRODUCTION

Since Grätzel reported the concept of electrochemical light absorption in order to produce electrons from photons in 1991 [1], the resulting dye-sensitized solar cells (DSSCs) have attracted

tremendous attention as a focus area in photovoltaics research thus far. Many researchers have attempted to enhance the performance of DSSCs to the level of solar cells based on inorganic materials such as amorphous silicon and chalcogenide compounds. In order to achieve a higher conversion efficiency for DSSCs, it is required to improve several key performance factors of DSSC devices such as the short-circuit current density ($J_{sc}$), open-circuit voltage ($V_{oc}$), and fill factor (*FF*).

Thus far, most of the research on DSSCs had focused on designing an n-type semiconductor to function as a working electrode [2-4], synthesis of novel light absorbent [5-7], and development of electrolytes [8-11] to attain high performance from the DSSCs through enhancement of the $J_{sc}$ or $V_{oc}$. However, in contrast with the other components, only a few studies focusing on the counter electrode have been reported, and they have mainly dealt with developing new catalytic materials, such as a series of carbon materials [12-15], inorganic compounds [16-18], and conducting polymers [19], for the sake of finding a substitute for platinum. A conducting layer for the formation of the counter electrode, however, is also important for enhancement of photoelectrical performance because of energy band alignment, electrical conductivity of the electrode, and formability of catalysts and their flexibility. Only a minority of the studies have dealt with the idea of using a conductor for the counter electrode.

Through a comparison of various flexible materials, both Fang et al. [20] and Ma et al. [21] reported that stainless steel (SS) is a strong candidate material, and additional study of SS was reported by Kim et al. and Yun et al. [22, 23]. DSSCs using SS coated with platinum (Pt) as a counter electrode, however, have relatively lower photocurrent conversion efficiency than conventional DSSCs with Pt-formed fluorine-doped tin oxide (FTO) as the counter electrode.

Recently, molybdenum (Mo) as electrode was used for double junction photo electrochemical cells based on iodine electrolyte in order to use an inorganic porous thin film as additional photocathode [24]. An application of Mo to conventional DSSCs, however, has not been reported or studied until now.

In this study, we found out that Mo is potential candidate for high performance DSSCs and report low-internal-resistance DSSCs using Mo as the conducting layer for the sake of the preparation of the counter electrode. Our results exhibited a high FF and photocurrent conversion efficiency because of the device's low electric resistance, better formability of Pt, and suitable work function for band alignment. For comparison, we have fabricated DSSCs with conventional FTO as the conducting layer. Moreover, we have investigated the origin of the improved performance through surface morphology analysis such as scanning electron microscopy and electrochemical analyses including cyclic voltammetry and impedance spectroscopy.

## 2. EXPERIMENTAL

### *2.1. Preparation of molybdenum thin film on glass substrate*

Molybdenum (Mo) thin film with a thickness of 500 nm was deposited on the soda lime glass substrates by DC magnetron sputtering using a rectangular Mo target (purity, 99.95%). The substrates were rotated during deposition for film uniformity. The deposition chamber was evacuated by turbo

molecular pump to a base pressure of $3\times10^{-7}$ Torr, and the argon partial pressure was controlled with an electrical pendulum valve system. Mo thin films were deposited at a pressure of 1 mTorr and a DC power of 600 W without substrate heating.

### *2.2. Fabrication of DSSCs*

The geometry of the DSSCs was a conventional sandwich configuration that consists of a working electrode and a counter electrode, and the space between the electrodes was filled with an electrolyte solution.

In order to prepare a working electrode, fluorine-doped tin oxide (FTO) for a conductive transparent electrode was purchased from Pilkington (~ 8 Ω /sq) and cleaned using the general cleaning process for electronic applications: ultrasonic treatment in detergent, deionized water, acetone, and 2-propanol in that order for 15 min for each at room temperature. The transparent and porous titanium oxide film was formed on the cleaned FTO substrate using 20-nm particle-size $TiO_2$ paste (Solaronix, T/SP) with the doctor-blade coating method twice. The coated $TiO_2$ film was sintered at 500°C in air for 60 min. In order to obtain a high degree of light-harvesting and prevent other optical effects such as reflection, a $TiO_2$ (Solaronix, R/SP) layer formed from 400-nm particles was coated on the sintered $TiO_2$ film. This formation process was the same as that for transparent and porous $TiO_2$ film. For the sake of a strong connection between the $TiO_2$ nanoparticles in the porous film, the $TiO_2$ film was treated by 40 mM $TiCl_4$ (Aldrich) for 30 min at 70°C in a dry oven, and then sintered at 500°C in air for 60 min again. For adsorption of N719 dye (Solaronix) as a photo-sensitizer, the $TiO_2$ film was immersed in 0.3 mM dye solution that consisted of a mixture of acetonitrile and tert-butanol (50:50 vol%) at room temperature. After 24 hours, the dye-adsorbed $TiO_2$ film was rinsed with acetonitrile and then dried at 70°C for about 10 min. The active area's length was 4 mm, and its width was 6 mm.

Counter electrodes based on Mo and FTO substrates were prepared by a chemical reduction method using sodium borohydride ($NaBH_4$) purchased from Aldrich. Mo and FTO substrates with 0.7 mm holes were coated with 7 mM chloroplatinic acid ($H_2PtCl_6$, Aldrich) solution as a Pt precursor was coated using the spin coating method. The spun-cast substrates were immersed in 60 mM $NaBH_4$ solution in order to form the Pt catalyst by reduction.

For the fabrication of DSSCs, Surlyn (Solaronix SX1170-60) with a thickness of 60 μm was used as a thermoplastic sealant in the role of a spacer between the working and counter electrodes. A liquid electrolyte was composed of 0.03 M iodine, 0.05 M lithium iodide, 1 M 1-methyl-3-propylimidazolium iodide, 0.1 M guanidine thiocyanate, and 0.5 M tert-butyl pyridine as components and 85% acetonitrile, 15% valeronitrile as the solvent. This electrolyte was injected into the interior of the cell through the holes. In order to minimize other effects, finalization of the cell's manufacturing process was finalized by masking it with black tape and without any soldering.

*2.3. Characterization of physical, electrochemical, and electrical properties*

The morphologies of bare and Pt-formed FTO and Mo substrates were measured using scanning electron microscopy (SEM, Hitachi S-4800II). An X-ray diffraction (XRD, PANalytical Empyrean) experiment was carried out to confirm the crystallinity of the Mo thin film.

A potentiostat (IVIUM, Iviumstat) was used for performing cyclic voltammetry (CV) measurements. The CV tests were performed in a three-electrode system (consisting of working, counter, and reference electrodes), and either Pt-formed FTO or Mo substrate, Pt mesh, and $Ag^+$/AgCl 1 M were used for the working, counter, and reference electrodes, respectively. The electrolyte was composed of 5 mM iodine ($I_2$, Aldrich) and 5 mM lithium iodide (LiI, Aldrich) in acetonitrile containing 0.1 M tetrabutylammonium hexafluoro phosphate (TBA-$PF_6$, Aldrich) as the supporting electrolyte. The voltage range of the data was from -0.6 V to +1.0 V with a scan rate of 50 mV/s.

The photocurrent-density–voltage characteristic of the DSSCs was measured using a Keithley 2400 source meter and a solar simulator equipped with a 1 kW xenon arc lamp (ORIEL, Newport). A standard silicon solar cell (PV Measurement Inc.) was used for calibration with the power of the AM 1.5 simulated light (100 mW/$cm^2$).

To perform electrochemical impedance spectroscopy (EIS), the DSSCs were measured under an AM 1.5 light condition by a potentiostat (IVIUM, Iviumstat); the frequency range was from 0.1 Hz to 100 kHz. The data obtained from this measurement was fitted by simulation software (Scribner Associates, Z-View), which proposed an equivalent circuit to model the data.

## 3. RESULTS AND DISCUSSION

To investigate the crystal orientation and work function of the Mo film grown directly on top of the soda lime glass, an X-ray diffraction measurement was carried out. The XRD peak at a 2 theta of 40.500° indicates that the crystal structure of the Mo film has the (110) face (inset in Figure 1). Berge et al. [25] have reported that the work function of the (110) face of Mo is 4.95±0.02 eV, which corresponds to the work function of FTO, 4.9 eV [26]. Therefore, replacing the FTO with Mo as the counter electrode material does not lead to negative effects such as an increase of the charge barrier, and we can more clearly verify the effect of using Mo as the counter electrode. In order to identify the surface morphology of the Pt catalyst formational properties on Mo and FTO, field-emission scanning electron microscopy (FE-SEM) was carried out on bare and Pt-formed FTO as well as bare and Pt-formed Mo. As shown in Figure 2, the grain size of Pt nanoparticles varied depending on the range of the counter electrode substrate. The size of the Pt nanoparticles on the FTO was about 5–10 nm, whereas that on the Mo was significantly larger (~50 nm). This formation might be attributed to the aggregation in order to reduce the surface energy during the chemical reduction process from the Pt precursor to the Pt nanoparticles [22, 23]. Generally, density of Pt particles on the FTO as counter electrode in conventional DSSCs is very low, which is sufficient to DSSCs operating. However, in this report, these sparse Pt particles on Mo, like this study, were formed larger than that on FTO. These large Pt nanoparticles on the Mo, which can cause higher catalytic properties and lower charge

transport resistance between Pt and the electrolyte because of large Pt boundary area, can provide a much greater chance of reaction on the Pt catalysts.

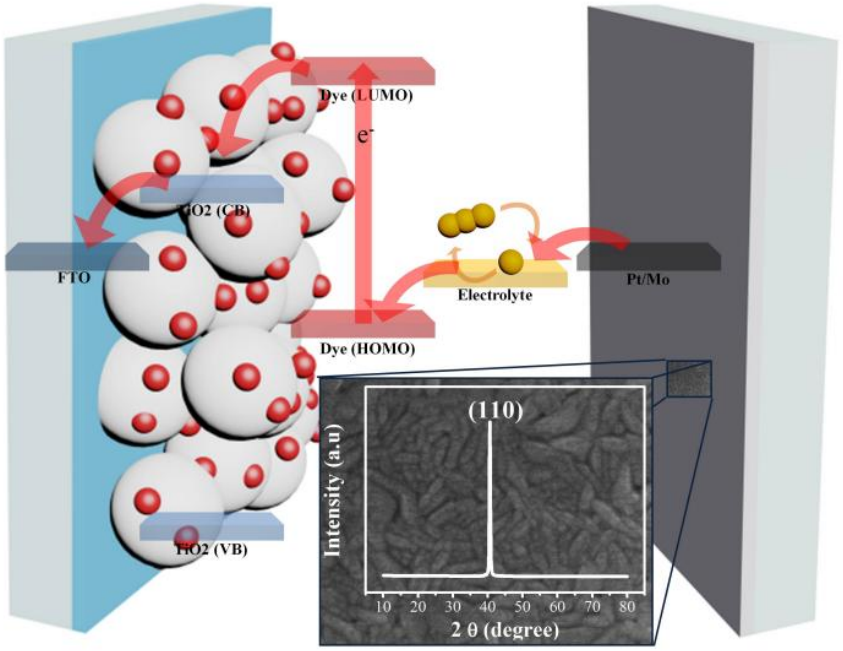


**Figure 1.** Geometry of DSSCs and scheme of the electron transport process using a band diagram. The inset consists of the SEM image and XRD pattern of bare Mo.

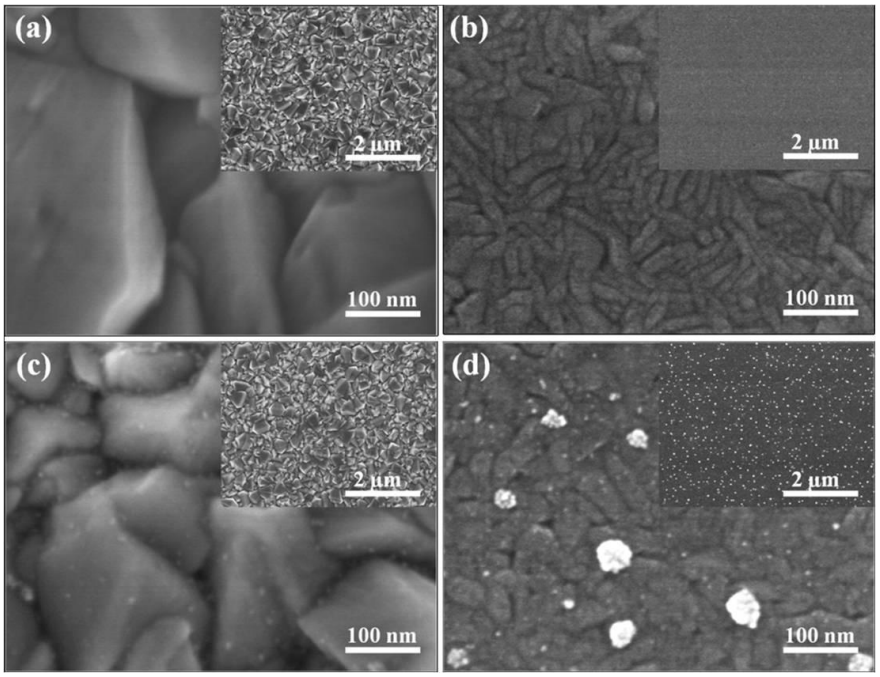


**Figure 2.** SEM images of (a) bare FTO, (b) bare Mo surface, (c) Pt-formed FTO, and (d) Pt-formed Mo surface

Figure 3 shows the cyclic voltammetry (CV) curve of Pt-formed FTO and Mo for the sake of the evaluation of catalytic activity. In this CV curve, two pairs of redox peaks were measured; the relatively negative pair was caused by redox reaction (1), and the relatively positive pair was due to redox reaction (2) [16-18].

$$I_3 + 2e^- \rightleftharpoons 3I^- \quad (1)$$

$$3I_2 + 2e^- \rightleftharpoons 2I_3^- \quad (2)$$

Generally, the counter electrode serves to catalyze the chemical reduction reaction of the tri-iodine ion to the iodide ion, and one of the parameters for evaluating the catalytic activity of the counter electrode is the peak current density because a high current at a fixed voltage value indicates the generation of a much stronger reaction [27, 28]. Another parameter is the peak-to-peak separation ($\Delta E_p$) because it is in inverse proportion to the electrochemical constant, $k_s$ ($\Delta E_p \propto 1/k_s$), and therefore the smaller the peak-to-peak separation is, the higher the catalytic properties are [14, 17].

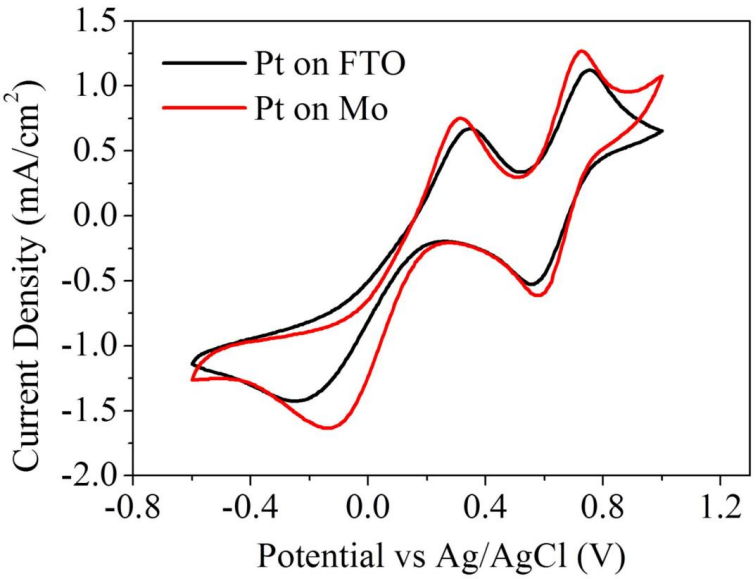


**Figure 3.** Cyclic voltammograms of Pt-coated FTO and Pt-coated Mo counter electrodes. The scan rate is 0.5mV/s.

Compared with the two counter electrodes, Pt-formed FTO and Mo, the case of the Mo electrodes exhibits a high current density, which means that it has higher electrochemical catalytic activity. The $\Delta E_p$ of the FTO and Mo counter electrodes are 590 mV and 450 mV, respectively. The FTO counter electrode has a higher $\Delta E_p$ value than the Mo counter electrode, which is evidence that the large Pt nanoparticles on the Mo cause it to have a high electrochemical constant ($k_s$); thus, replacement of the FTO counter electrode with a Mo counter electrode can reduce the internal resistance and then enhance the photocurrent conversion efficiency of the DSSCs.

Through the current density-voltage electrical characteristics of the DSSCs using Pt-formed FTO and Mo as the counter electrode (which we refer to as device_FTO and device_Mo, respectively)

under the 100mW/cm$^2$, the effect of replacing FTO by Mo was confirmed (Figure 4). The two resulting solar cells have short circuit current densities that are similar (Device_FTO: 16.089 mA/cm$^2$, Device_Mo: 15.917 mA/cm$^2$), and the same is true for the open circuit voltage (Device_FTO: 0.705 V, Device_Mo: 0.698 V). The observed difference in FF values between the two cells, however, was noticeable and had an influence on different photocurrent conversion efficiencies of device_FTO and device_Mo (Device_FTO: 64.62 %, Device_Mo: 69.63 %). Indeed, as shown in the Figure 4 and the Table 1, device_Mo had a higher FF than device_FTO; thus, the photocurrent conversion efficiency shows the same tendency for the FF in the tests on this cell (Device_FTO: 7.33 %, Device_Mo: 7.74 %).

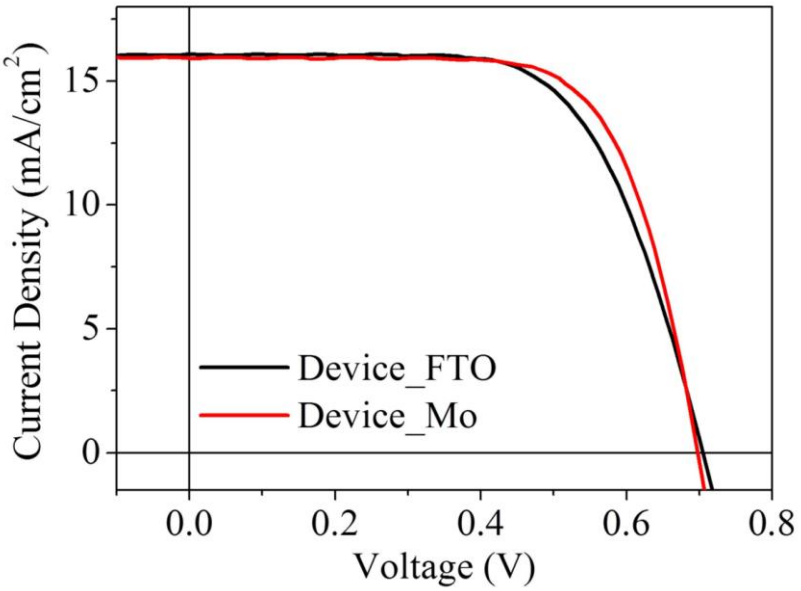


**Figure 4.** An electrical characteristic of Device_FTO and Device_Mo measured under 100mW/cm$^2$ (1 sun condition)

**Table 1.** Photovoltaic parameters of Device_FTO and Device_Mo

| Sample | $V_{oc}$ (V) | $J_{sc}$ (mA/cm$^2$) | *FF* (%) | $\eta$ (%) |
|---|---|---|---|---|
| Device_FTO | 0.705 | 16.089 | 64.62 | 7.33 |
| Device_Mo | 0.698 | 15.917 | 69.63 | 7.74 |

In order to determine this enhancement of the FF and the photocurrent conversion efficiency by replacing FTO with Mo as the conductor for the counter electrode, electrochemical impedance spectroscopy (EIS) experiments were carried out on the devices in the frequency range of 0.1 Hz–100 kHz under a 1.5 AM light condition. Generally, the conventional three semicircles in the Nyquist plot indicate the internal resistance of devices. The series resistance ($R_s$) of the cells was estimated from the intercept on the real axis at the highest frequency; the first arc in the high frequency range indicates the electrochemical reaction resistance or redox couple at the Pt counter electrode ($R_{ct1}$); the second arc in

the intermediate frequency range demonstrates the charge recombination resistance at the interface between the $TiO_2$ and the electrolyte ($R_{ct2}$); and the third arc was caused by Warburg diffusion of the redox species ($W_s$). Recently, although additional factors that cause EIS spectra have been suggested by a variety of research efforts, these interpretations are conventional and have been accepted as before, although they do not show any significant difference from recently suggested explanations.

Figure 5 illustrates the origin of the difference in electric properties between the devices using FTO and Mo electrodes. First, the dissimilarity of the sheet resistance between FTO (8.2 Ω/sq) and Mo (0.16 Ω/sq) has brought about the difference in $R_s$ between device_FTO and device_Mo, 15.11 Ω•cm$^2$ and 7.25 Ω•cm$^2$, respectively. In addition, the decrease of the $R_{ct1}$ value from 6.87 Ω•cm$^2$ to 3.14 Ω•cm$^2$ by replacing the FTO counter electrode with a Mo counter electrode was induced by the higher redox reactivity of Pt on Mo than that on FTO.

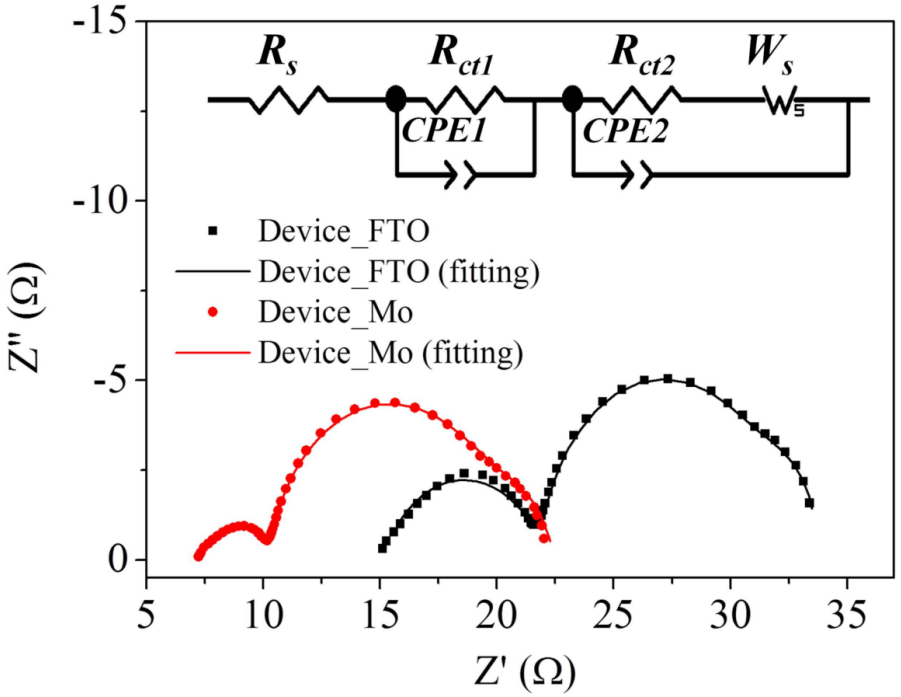


**Figure 5.** Nyquist plots of Device_FTO and Device_Mo. The inset indicates an equivalent circuit model used for the devices in this study.

## 4. CONCLUSION

In summary, we fabricated dye-sensitized solar cells using Pt-coated Mo as a counter electrode in order to achieve a high photocurrent conversion efficiency through enhancement of the FF. Replacing FTO with Mo has brought about decreases in the series resistance of DSSCs because of the low sheet resistance of Mo and the catalytic reactivity enhancement of the counter electrode through formation of larger Pt nanoparticles on the Mo. Therefore, this substitution has induced successive decreases in the internal resistance and an increase in FF; thus, the photocurrent conversion efficiency

has increased also. Overall, this study suggests that the Pt-coated Mo is a strong potential candidate as a counter electrode for elevating the performance of dye-sensitized solar cells to new heights. Furthermore, our approach has the potential to deliver high-quality flexible dye-sensitized solar cells because of the flexibility of the metals.

ACKNOWLEDGMENT
This work was supported by a grant from the Fundamental R&D program for Core Technology of Materials (10037239) funded by the Ministry of Knowledge Economy, Republic of Korea, and by the DGIST R&D Program of the Ministry of Education, Science and Technology of Korea (13-EN-04).

**References**

1. B. O'Regan and M. Gratzel, *Nature*, 353 (1991) 737
2. X. Feng, K. Zhu, A.J. Frank, C.A. Grimes and T.E. Mallouk, *Angewandte Chem*., 124 (2012) 2781
3. S. H. Ko, D. Lee, H. W. Kang, K. H. Nam, J. Y. Yeo, S. J. H, C.P. Grigoropoulos and H.J. Sung, *Nano Lett*., 11 (2011) 666
4. Y.-H. Lin, Y.-C. Wu and B.-Y. Lai, *Int. J. Electrochem. Sci*., 7 (2012) 9478
5. S. Qu, C. Qin, A. Islam, Y. Wu, W. Zhu, J. Hua, H. Tian and L. Han, *Chem. Commun*., 48 (2012) 6972
6. X. Jiang, K.M. Karlsson, E. Gabrielsson, E.M.J. Johansson, M. Quintana, M. Karlsson, L. Sun, G. Boschloo and A. Hagfeldt, *Adv. Funct. Mater*., 21 (2011) 2944
7. A. Dualeh, F.D. Angelis, S. Fantacci, T. Moehl, C. Yi, F. Kessler, E. Baranoff, M.K. Nazeeruddin and M.Gratzel, *J. Phys. Chem. C*, 116 (2012) 1572
8. J. Yum, E. Baranoff, F. Kessler, T. Moehl, S. Ahmad, T. Bessho, A. Marchioro, E. Ghadiri, J. Moser, C. Yi, M.K. Nazeeruddin and M. Grätzel, *Nature Commun*., 3 (2012) 631
9. T. Daeneke, Y. Uemura, N.W. Duffy, A.J. Mozer, N. Koumura, U. Bach and L. Spiccia, *Adv. Mater*. 24 (2012) 1222
10. J. Burschka, V. Brault, S. Ahmad, L. Breau, M.K. Nazeeruddin, B. Marsan, S.M. Zakeeruddin and M. Gratzel, *Energy Environ. Sci*., 5 (2012) 6089
11. S.-Y. Ku and S.-Y. Lu, *Int. J. Electrochem. Sci*., 6 (2011) 5219
12. J. Velten, A.J. Mozer, D. Li, D. Officer, G. Wallace, R. Baughman and A. Zakhidov, *Nanotechnology*, 23, (2012) 085201
13. S. Huang, Z. Yang, L. Zhang, R. He, T. Chen, Z. Cai, Y. Luo, H. Lin, H. Cao, X. Zhu and H. Peng, *J. Mater. Chem.*, 22 (2012) 1683
14. E. Ramasamy and J. Lee, *Carbon*, 48 (2010) 3715
15. 15.K.-C. Lin, J.-Y. Huang and S.-M. Chen, *Int. J. Electrochem. Sci*., 7 (2012) 12786
16. M. Wu, Q. Zhang, J. Xiao, C. Ma, X. Lin, C. Miao, Y. He, Y. Gao, A. Hagfeldt and T. Ma, J. *Mater. Chem*., 21 (2011) 10761
17. F. Gong, H. Wang, X. Xu, G. Zhou and Z. Wang, *J. Am. Chem. Soc*., 134 (2012) 10953
18. W. Chi, J. Han, S. Yang, D. Roh, H. Lee and J. Kim, *Chem. Commum*., 48 (2012) 9501
19. S. Peng, J. Liang, S.G. Mhaisalkar and S. Ramakrishna, *J. Mater. Chem*., 22 (2012) 5308
20. X. Fang, T. Ma, M. Akiyama, G. Guan, S. Tsunematsu and E. Abe, *Thin Solid Films*, 472 (2005) 242
21. T. Ma, X. Fang, M. Akiyama, K. Inoue, H. Noma and E. Abe, *J. Electroanal. Chem*., 574 (2004) 77
22. J. Kim and S. Rhee, *J. Electrochem. Soc*., 159 (2012) B6
23. J. Yun, T. Kim, S. Cho, K. Hwang, J. Lee, H. Gu and K. Park, *J. Sci. Conf. Proc*., 1 (2009) 6

24. P. Dai, G. Zhang, Y. Chen, H. Jiang, Z. Geng, Z. Lin and J. Zhan, *Chem. Commun*. 48 (2012) 3006
25. S. Berge, P.O. Gartland and B.J. Slagsvold, *Surf. Sci*., 43 (1974) 275
26. X. Wei, T. Xie, D. Xu, Q. Zhao, S. Pang and D. Wang, *Nanotechnology* 19 (2008) 275707
27. V. Dao, S. Kim, H. Choi, J. Kim, H. Park and J. Lee *J. Phys. Chem. C*, 115 (2011) 25529
28. J. Lin, J. Liao and T. Hung, *Electrochem. Commun*., 13 (2011) 977

© 2013 by ESG (www.electrochemsci.org)